



Enhancing Drug Utilization Efficiency via Dish-Structured Triboelectric Nanogenerator

Qu Chen^{1,2}, Wenjing Deng³, Jingjin He², Li Cheng^{4*}, Pei-Gen Ren^{5,6*} and Yang Xu^{3*}

¹Institute of Biomedicine and Biotechnology, Shenzhen Institute of Advanced Technology, Chinese Academy of Sciences, Shenzhen, China, ²Shenzhen International Institute for Biomedical Research, Shenzhen, China, ³School of Basic Medical Sciences, Southern Medical University, Guangzhou, China, ⁴School of Materials and Energy, Lanzhou University, Lanzhou, China, ⁵Center for Energy Metabolism and Reproduction, Shenzhen Institute of Advanced Technology, Chinese Academy of Sciences, Shenzhen, China, ⁶Shenzhen College of Advanced Technology, University of Chinese Academy of Sciences, Shenzhen, China

OPEN ACCESS

Edited by:

Qitong Huang,
Gannan Medical University, China

Reviewed by:

Xiang-Yu Kong,
Technical Institute of Physics and
Chemistry (CAS), China
Guangqin Gu,
Henan University, China

*Correspondence:

Li Cheng
chengl2007@live.cn
Pei-Gen Ren
pg.ren@siat.ac.cn
Yang Xu
yangxu@ucsd.edu

Specialty section:

This article was submitted to
Nanobiotechnology,
a section of the journal
Frontiers in Bioengineering and
Biotechnology

Received: 22 May 2022

Accepted: 06 June 2022

Published: 06 July 2022

Citation:

Chen Q, Deng W, He J, Cheng L,
Ren P-G and Xu Y (2022) Enhancing
Drug Utilization Efficiency via Dish-
Structured
Triboelectric Nanogenerator.
Front. Bioeng. Biotechnol. 10:950146.
doi: 10.3389/fbioe.2022.950146

Due to the finding of severe side effects and low therapeutic efficacy with cancer chemotherapy, there still remains a great challenge to benefit patients with curative effect. In this work, we designed a self-powered drug delivery system comprising a current source derived from the disk TENG (D-TENG) and a pair of Au electrodes. Thus, cells seeded within the electrode gap could be stimulated by the current followed by D-TENG's work. Under the rotation frequency of about 7.4 Hz, the peak output current and voltage of the D-TENG reached 3.7 μ A and 135 V and achieved an average of 2.8 μ A of output current. Furthermore, the D-TENG also showed its good stability to output steady current in a long-term condition. When applying the electric stimulation by this self-powered drug delivery system, a chemotherapy drug, doxorubicin (DOX), had significant uptake by cancer cells. Therefore, utilizing a novel TENG device as a part of chemotherapy would provide a new opportunity in future disease treatment.

Keywords: doxorubicin, dish-structure, triboelectric nanogenerator, drug utilization, enhanced efficiency

1 INTRODUCTION

Despite extensive efforts worldwide, cancer remains one of the leading causes of mortality (Sung et al., 2021). Surgery or radiotherapy is an effective strategy for the treatment of local tumors. In the remaining cases, chemotherapy is the main priority in cancer treatment (Chu and Sartorelli, 2018). However, chemotherapy is always accompanied by severe side effects and low therapeutic efficacy (Zhong et al., 2021). For example, a first-line clinical drug, doxorubicin (DOX) (Hai-wen et al., 2013), has been reported to result in all kinds of toxic side effects, including cardiotoxicity and alopecia, due to its low uptake by cancer cells (Zhao et al., 2019). Therefore, developing a new technology to enhance drug utilization is extremely urgent in order to reduce the side effects and improve efficacy.

Considering the physiological roles of bioelectrical signals in cell biology, electrical stimulation (ES) was introduced to improve some operations in many biological scenes. For example, a well-known microbiology technique called electroporation takes advantage of an electrical field to change the permeability of the cell membrane, allowing biomolecule transportation or even cell fusion (Zhang et al., 2018). Recently, ES has been demonstrated to have the potential to be a promising strategy for drug delivery and therapy. Karan Gulati's group combining electrical drug delivery and electrical stimulation therapy achieved beneficial results in bone implantation (Gulati et al., 2016). Cassandra L. Weaver's group developed a drug delivery nanocomposite controlled by electricity to meet various therapeutic needs (Weaver et al., 2014). With the concerted efforts of Pei-Chi Lee and

his colleagues, increased nanomedicine accumulation within tumor tissue stimulated by electrical single-walled carbon nanotubes helps to delay tumor growth (Lee et al., 2016). However, most of these techniques require an external power source, greatly increasing the cost and inconvenience, thereby limiting their further application.

Triboelectric nanogenerators (TENGs) (Fan et al., 2012a; Wang et al., 2014a; Zheng et al., 2014; Cheng et al., 2018; Qin et al., 2020; Zhang et al., 2020; Zhang et al., 2021a), which were invented to harvest unordered ambient mechanical energy on the basis of triboelectric effect and Maxwell's displacement current (Wang, 2017), have been proved to be a simple, low-cost, and portable power source for self-powered devices and systems (Wang, 2013; Zheng et al., 2016; Cheng et al., 2017; Wang et al., 2018; Hao et al., 2021; Shang et al., 2021; Wang et al., 2021). A series of methods were investigated to increase the output performance of TENGs, such as material selection (Wang, 2013), surface roughness increment (Fan et al., 2012b; Zhang et al., 2015), surface charge injection (Wang et al., 2014a; Wang et al., 2014b), charge pump method (Cheng et al., 2018), step-down circuit (Qin et al., 2018), and multiple channel method (Zhang et al., 2022a). As a result, TENG's output voltage and peak current have been increased to more than ten thousand volts (Li et al., 2021) and hundreds of milliamperes (Cheng et al., 2013), and its output charge density is up to millicoulombs per square meter (Zhang et al., 2022a). As the output has been ameliorated to a very high level, TENGs are widely applied to establish self-powered nanodevices or nanosystems. For example, TENG's

output changed under different driving forces, making it available to sense and detect these applied forces (Chen et al., 2022); through connecting TENGs together with sensors, UV light intensity, gas concentration, and other environmental information could be detected to realize the application of self-powered detection (Zheng et al., 2014; Su et al., 2018; Zhao et al., 2018; Zheng et al., 2022); using the current generated by TENGs, self-powered anticorrosion was realized (Wang et al., 2014a). Furthermore, through the use of display units or wireless transmission technology, the sensing result could be displayed directly or sent out for further processing (Zheng et al., 2014; Cheng et al., 2017; Zhang et al., 2022b). Using TENGs as a power source, many medical applications have been developed (Zhang et al., 2021b), and several self-powered systems have been designed for drug delivery (Wang et al., 2016; Bok et al., 2018; Liu et al., 2019). Among these systems, nanoneedles are considered one of the most effective methods for drug delivery, but bring up two problems: first, the active electrical area is usually very small, which makes it difficult to stimulate enough cells for therapy; second, fabrication of the nanoneedles and extra devices is always complicated and expensive. Thus, a simple and self-powered delivery system is required for current medicines.

In this work, we designed a very simple self-powered drug delivery system in order to reduce the severe side effects and enhance the therapeutic efficacy of chemotherapy. In this system, a disk TENG (D-TENG) is designed to provide a stable current, which performs the electrical stimulation towards cells/tissues

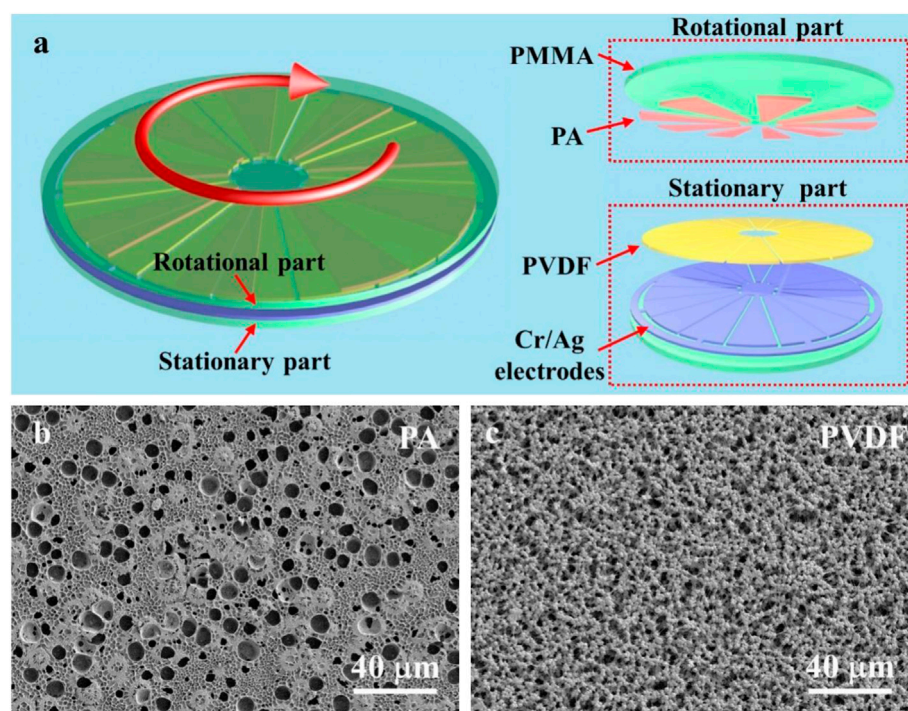


FIGURE 1 | Design of the D-TENG. **(A)** Schematic diagram of the D-TENG. **(B)** Scanning electron microscope (SEM) image of the spin-coated PA film. **(C)** SEM image of the spin-coated PVDF film.

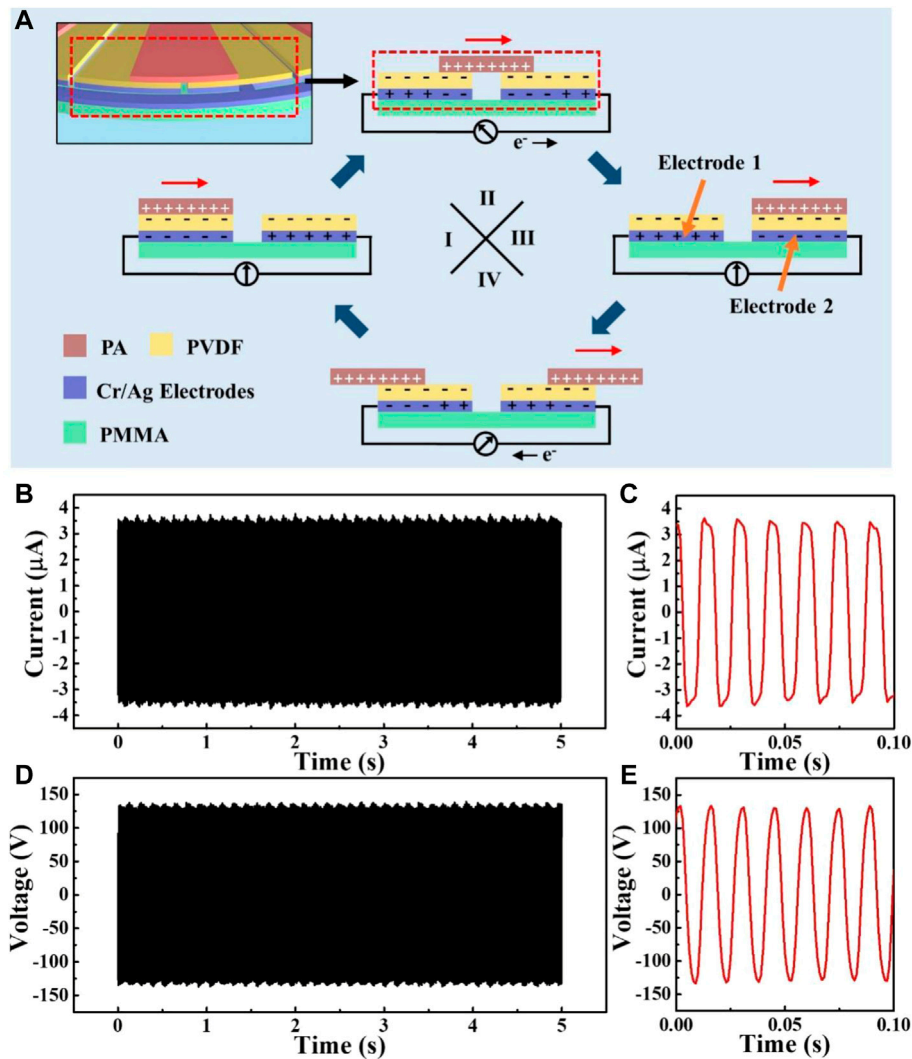


FIGURE 2 | Output of the D-TENG. **(A)** Schematic diagram of the working mechanism of the D-TENG. **(B)** Output current of the D-TENG. **(C)** Enlarged view of D-TENG's output current. **(D)** Output voltage of the D-TENG. **(E)** Enlarged view of D-TENG's output voltage.

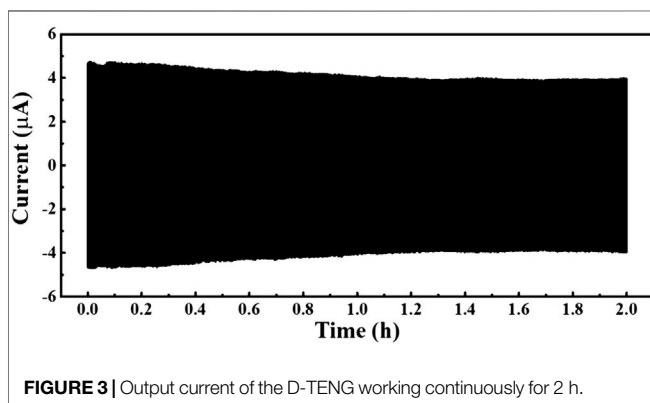


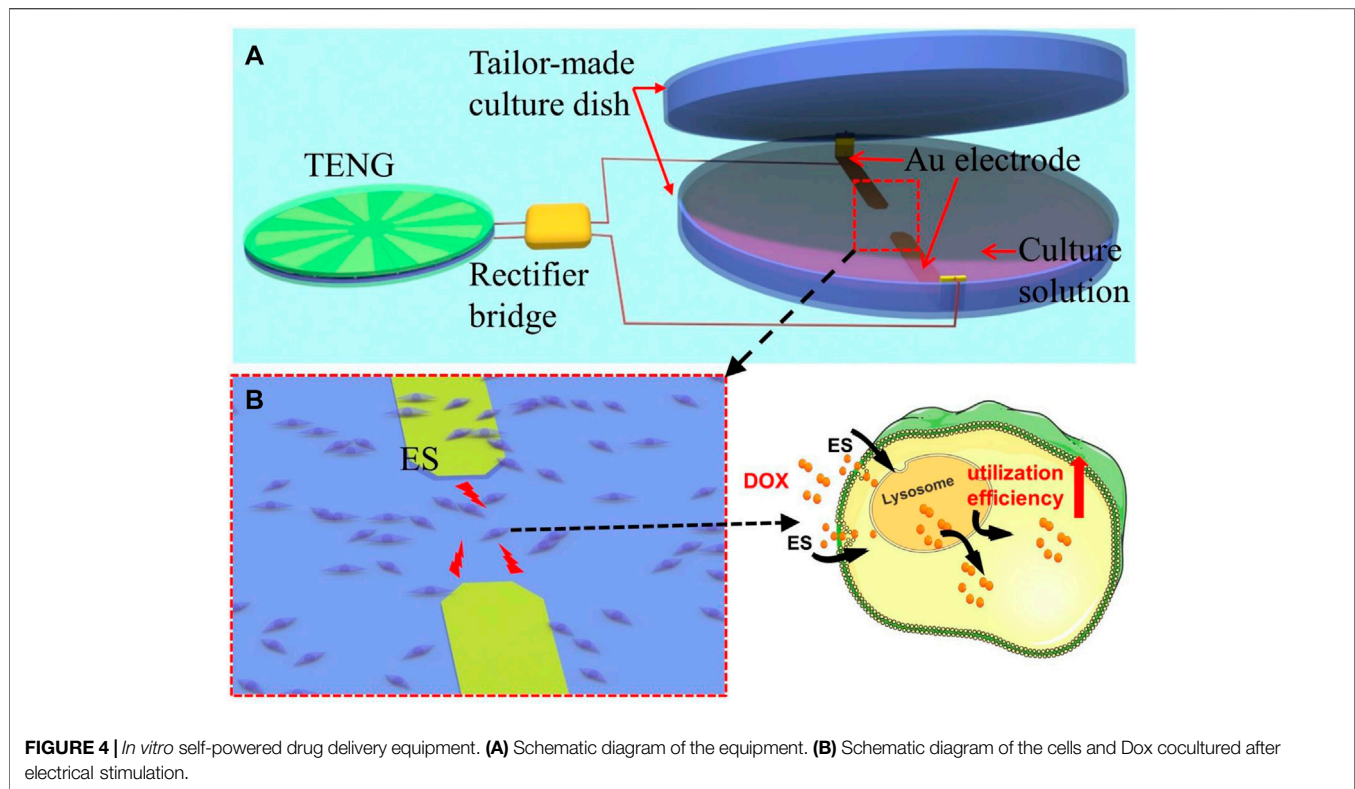
FIGURE 3 | Output current of the D-TENG working continuously for 2 h.

within two Au electrodes. An *in vitro* experiment showed that using this self-powered drug delivery system, the utilization efficiency of Dox was effectively increased.

2 MATERIALS AND METHODS

2.1 Materials

DOX was provided by Aladdin (Hangzhou, China). Mouse breast cancer cells (4T1 cell line) were purchased from the American Type Culture Collection (ATCC). PVDF powder was provided by Alfa Aesar (Shanghai, China). PA powder was provided by Macklin (Shanghai, China). All organic solvents were provided by Sinopharm Chemical Reagent (Shanghai, China).



2.2 Preparation of PA and PVDF Solutions (Weaver et al., 2014)

To prepare the PA solution, 2 g of PA powder was added to 16 g of formic acid and then stirred for 30 min to make the PA powder dissolve. To prepare the PVDF solution, 3.75 g of PVDF powder was added to 8.5 g of N,N-dimethylacetamide (DMAC) and 12.75 g of acetone and then stirred at 60°C for 30 min to make the powder dissolve.

2.3 Fabrication of the D-TENG

Two pieces of PMMA sheet were first cleaned in sequence with ethanol and deionized water. The PA solution was spin-coated on one of the PMMA sheets at a speed of 1500 rpm for 60 s and then left for 30 min to make sure the solution is dry. The sheet was cut into the needed shape with 3 cm of radius to make the rotational part of the D-TENG. On the other piece of the PMMA sheet, Cr and Ag films were sputtered on one surface to make the Cr/Ag electrode, and PVDF solution was spin-coated on the Cr/Ag film at the speed of 1500 rpm for 60 s and then left for 30 min to make sure the solution is dry. The sheet was then cut into the needed shape; in this process, the Cr/Ag electrode was cut into two pieces, as shown in **Figure 1A** and two copper wires were connected to the two electrodes to make the stationary part of the D-TENG. At last, two parts of the D-TENG were assembled with the PA film in contact with the PVDF film and the center of the sheets aligned.

2.4 Fabrication of the Tailor-Made Culture Dish With Au Electrodes

Au electrodes with the needed shape were sputtered on the inner side of the bottom of an ordinary culture dish. Then, two copper wires were connected to the Au electrodes at the edge of the dish to make sure only the Au electrodes will contact the culture solution. The prepared culture dish with Au electrodes was sterilized with medicinal alcohol and UV light before cell culture.

2.5 Flow Cytometric Analysis of Drug Utilization Efficiency

4T1 cells were seeded in plates (3×10^5 cells/well) and cultured overnight. On the second day, media was changed and replaced with fresh media containing DOX. Cells were treated with/without TENG current stimulus for 1 h. The cells treated without DOX or ES were used for the control. 4T1 cells were cultured for another 24 h. Then, the cells were harvested and analyzed by a flow cytometer (BD Biosciences).

3 RESULTS AND DISCUSSION

As **Figure 1A** shows, the D-TENG comprises a rotational part and a stationary part. The rotational part contains a PMMA sheet as the substrate and nine PA films which act as a kind of friction layer and are attached to the PMMA sheet. The PA films are cut into circular sectors and ring-distributed on the PMMA sheet

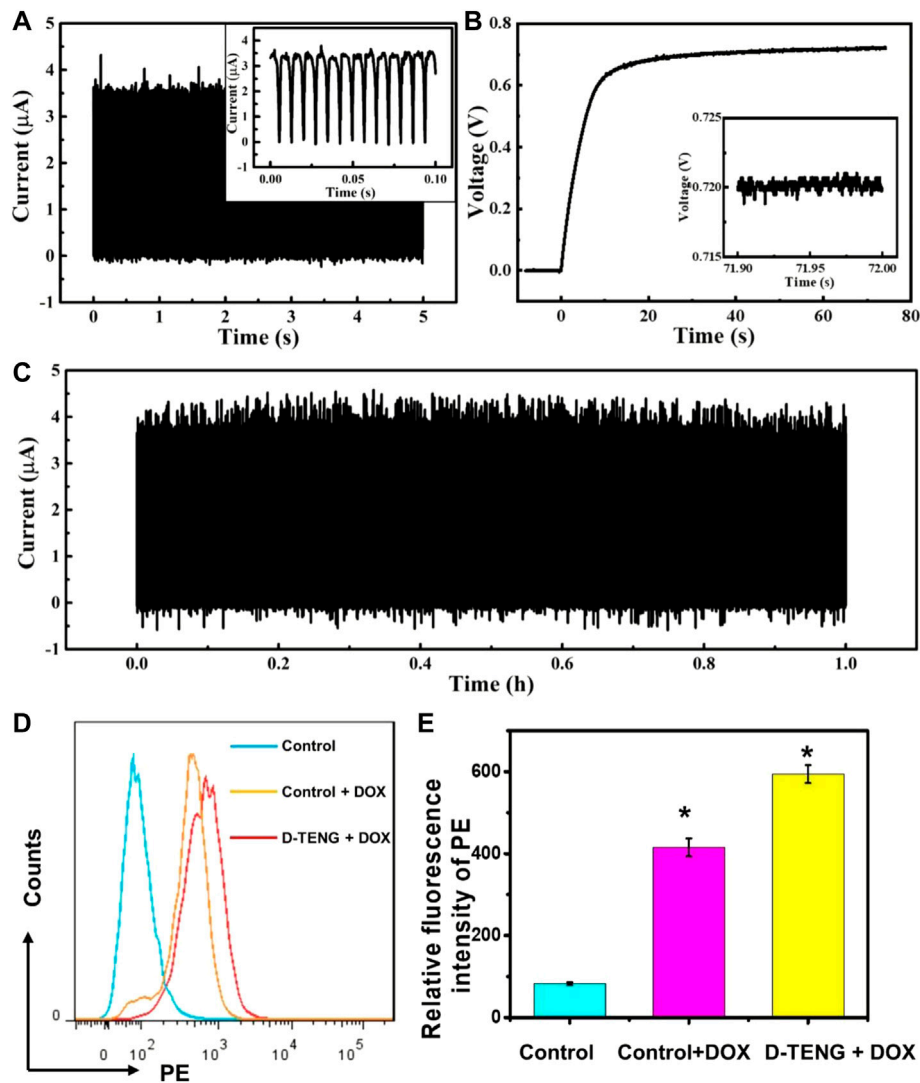


FIGURE 5 | *In vitro* enhancing drug utilization efficiency. **(A)** The current transmitted to the tailor-made culture dish. **(B)** The voltage between the Au electrodes. **(C)** The current is transmitted to the tailor-made culture dish in the simulation process. **(D)** The uptake efficiency of 4T1 cells for Dox under 1 h stimulation was analyzed 24 h after stimulation. **(E)** Quantitative analysis of **(D)**. Unpaired *t* test. $n = 3$, * $p < 0.05$, ns represents no significant difference.

with sectorial spaces of the same size. The stationary part contains a PMMA sheet as the substrate, two Cr/Ag electrodes and the sectorial PVDF films which act as the other kinds of friction layers attached to the electrodes. Each electrode contains nine sectorial units with the same size and distribution as the PA films. So, when the D-TENG is rotated, the PA films overlap with two electrodes alternately. To clearly observe the materials coating in the D-TENG, PA films (**Figure 1B**) and PVDF films (**Figure 1C**) were characterized using the scanning electron microscope (SEM). As the picture shows, rough surfaces with holes or particles formed naturally in the fabrication process of the films will help to increase the performance of the D-TENG. Details of the fabrication process are shown in the methods.

Figure 2A shows the working mechanism of the D-TENG. When the rotational part is rotated, PA films slide across the PVDF films. In this process, PA films rub with PVDF films. As a

result, PA films take positive charges and PVDF films take negative charges. The total area of the PVDF films is twice that of the PA films', and charge density of the PA films is twice of the PVDF films'. When PA films overlap with electrode 1 (state I), though the positive charge on the PA film is partly offset by the negative charge, the residual charge will induce a negative charge in electrode 1. At electrode 2, the negative charge taken by the PVDF films on its surface will induce a positive charge in it. As a result, electrode 1 will take a negative charge and electrode 2 will take a positive charge. When PA films slide from electrode 1 to electrode 2 (state II), the overlapping area of electrode 1 with the PA films decreases, the overlapping area of electrode 2 increase, and electrons move from electrode 1 to electrode 2 through the external circuit and generate current in the circuit. When the PA films overlap with electrode 2 (state III), electrode 1 takes a positive charge and electrode 2 takes a negative charge.

And when PA films slide from electrode 2 to electrode 1 (state 4), electrons move from electrode 2 to electrode 1 and generate reversed current in the circuit. So, following the D-TENG work, one round from states I to IV will continue to the next round, which periodically generates alternating current in the circuit. As there are nine sectorial PA films in the device, each revolution of the D-TENG will generate nine forward and nine reversed current peaks in the circuit.

The D-TENG's output was then measured with a rotational frequency of about 7.4 Hz. Its output current was about 3.7 μA (Figures 2B,C), and its output voltage was about 135 V (Figures 2D,E). The frequency of the output current and voltage was about 67 Hz, which was about nine times the D-TENG's driving frequency. The integral results (Supplementary Figure S1) showed that the transferred charge of each peak was about 21 nC, and the D-TENG could export 2.8 μC in one second. This indicated the average output current of the D-TENG was about 2.8 μA , which achieved the comparable level commonly used in cell electrical stimulation (Macfelda et al., 2017; Yuan et al., 2021).

As a source of energy, the stability of the D-TENG is one of the most important properties. Figure 3 shows the output current of the D-TENG working continuously for 2 hours. As expected, D-TENG's output decreased slightly in the first 1 hour, until its output current stabilized at about 4 μA . This good stability and intensity indicate the D-TENG has its own superiority for self-powered drug delivery.

Using this D-TENG as a power source, we designed a simple self-powered electrical stimulation system. The system contains the D-TENG, a rectifier bridge to convert the D-TENG's alternate current to direct current, and two Au electrodes to deliver the current. The Au electrode is used to prevent the possible electrochemical reaction. The cells/tissues stimulated by the current will increase the drug uptake efficiency.

An *in vitro* self-powered drug delivery experiment was then performed to check the effect of drug delivery using the simple drug delivery system. Figure 4A shows the equipment used in the *in vitro* experiment. In this equipment, the Au electrodes were deposited on the inner side of an ordinary culture dish (which consists of the tailor-made culture dish marked in the picture), which was used to culture and simulate the cells. Once the D-TENG is working, cells grow in the area between the two electrodes, which will be simulated. Figure 4B shows the mouse breast cancer cells (4T1 cell line) and Dox were cocultured in self-powered electrical stimulation system; after electrical stimulation, the uptake efficiency of cells for Dox will be determined.

In this experiment, mouse breast cancer cells (4T1 cell line) were seeded in culture plates. These cells were divided into three groups, including control, control with DOX (with no current stimulus), and D-TENG with DOX groups. In D-TENG with DOX groups, during the D-TENG 1 h continuous stimulation, the current transmitted to the tailor-made culture dish and the voltage between the Au electrodes were measured (Figures 5A,B). The D-TENG's output current was converted to direct current with a peak current of 3.5 μA and an average current of 2.9 μA (shown in Supplementary Figure S2). The voltage

between the Au electrodes increases rapidly in the first 10 s and stabilizes at 0.72 V. Figure 5C shows that the current was stable during the stimulation process. Afterwards, 4T1 cells were cultured for another 24 h, and the cells were harvested and analyzed by flow cytometer (BD Biosciences). The flow cytometric results indicated that this self-powered drug delivery system could significantly improve the utilization efficiency of Dox (Figures 5D,E). Therefore, the electrical stimulation of D-TENG might be used to improve drug utilization efficiency for disease treatment in the future.

In conclusion, we designed a very simple self-powered drug delivery system that contains a D-TENG, a rectifier bridge, and two Au electrodes. At a working frequency of about 7.4 Hz, the D-TENG generates a peak current of 3.7 μA and an average output current of 2.8 μA . Considering the wide ranges were applied in previous works, the output of the D-TENG is powerful enough to stimulate the cells. Also, the D-TENG has good performance to provide stable current for a long time. The output current of the D-TENG is converted to direct current by the rectifier bridge to stimulate the cells/tissues between the Au electrode. An *in vitro* experiment showed this self-powered drug delivery system could significantly improve the utilization efficiency of Dox. The next step is to establish a biocompatible system to meet the wearable or transplantable needs in clinical trials. Taken together, we developed a stable and powerful D-TENG system for drug delivery, which will be part of chemotherapy in future treatment.

DATA AVAILABILITY STATEMENT

The raw data supporting the conclusions of this article will be made available by the authors without undue reservation.

AUTHOR CONTRIBUTIONS

P-GR, YX, and LC were responsible for the conceptualization. QC and LC designed the methodology. LC provided the scientific guidance for the experiment. QC, WD, and JH contributed to most of the biological studies, and LC to fabrication and characterization. The manuscript was organized and written by QC and LC and revised by JH, P-GR, and YX. All authors read and approved the final version.

FUNDING

This work was supported by the Shenzhen Science and Technology Program (no. JCYJ20210324122214039) and the National Natural Science Foundation of China (no. 52172203).

ACKNOWLEDGMENTS

The authors would like to thank the Yuan lab for providing the experimental platform.

SUPPLEMENTARY MATERIAL

The Supplementary Material for this article can be found online at <https://www.frontiersin.org/articles/10.3389/fbioe.2022.950146/full#supplementary-material>

REFERENCES

- Bok, M., Lee, Y., Park, D., Shin, S., Zhao, Z.-J., Hwang, B., et al. (2018). Microneedles Integrated with a Triboelectric Nanogenerator: an Electrically Active Drug Delivery System. *Nanoscale* 10, 13502–13510. doi:10.1039/c8nr02192a
- Chen, Y., Gao, Z., Zhang, F., Wen, Z., and Sun, X. (2022). Recent Progress in Self-powered Multifunctional E-skin for Advanced Applications. *Exploration* 2, 20210112. doi:10.1002/EXP.20210112
- Cheng, G., Lin, Z.-H., Lin, L., Du, Z.-L., and Wang, Z. L. (2013). Pulsed Nanogenerator with Huge Instantaneous Output Power Density. *ACS Nano* 7, 7383–7391. doi:10.1021/nn403151t
- Cheng, L., Xu, Q., Zheng, Y., Jia, X., and Qin, Y. (2018). A Self-Improving Triboelectric Nanogenerator with Improved Charge Density and Increased Charge Accumulation Speed. *Nat. Commun.* 9, 3773. doi:10.1038/s41467-018-06045-z
- Cheng, L., Zheng, Y., Xu, Q., and Qin, Y. (2017). A Light Sensitive Nanogenerator for Self-Powered UV Detection with Two Measuring Ranges. *Adv. Opt. Mater.* 5, 1600623. doi:10.1002/adom.201600623
- Chu, E., and Sartorelli, A. (2018). Cancer Chemotherapy. *Lange's Basic Clin. Pharmacol.*, 948–976. <https://accessmedicine.mhmedical.com/content.aspx?bookid=2249§ionid=175224452>.
- Fan, F.-R., Lin, L., Zhu, G., Wu, W., Zhang, R., and Wang, Z. L. (2012). Transparent Triboelectric Nanogenerators and Self-Powered Pressure Sensors Based on Micropatterned Plastic Films. *Nano Lett.* 12, 3109–3114. doi:10.1021/nl300988z
- Fan, F.-R., Tian, Z.-Q., and Lin Wang, Z. (2012). Flexible Triboelectric Generator. *Nano Energy* 1, 328–334. doi:10.1016/j.nanoen.2012.01.004
- Gulati, K., Maher, S., Chandrasekaran, S., Findlay, D. M., and Lolic, D. (2016). Conversion of Titania (TiO₂) into Conductive Titanium (Ti) Nanotube Arrays for Combined Drug-Delivery and Electrical Stimulation Therapy. *J. Mat. Chem. B* 4, 371–375. doi:10.1039/c5tb02108a
- Hai-wen, Z., Li-qun, W., and Hong-liang, J. (2013). Chitosan-Based Cationic Micelles for Co-incorporation of Two Types of Drugs with Distinct Hydrophilicity. *Acta Polym. Sin.* 012, 1491–1499. doi:10.3724/SP.J.1105.2012.12115
- Hao, M., Zhang, R., Jia, X., Gao, X., Gao, W., Cheng, L., et al. (2021). A Polymer Based Self-Powered Ethanol Gas Sensor to Eliminate the Interference of Ultraviolet Light. *Sensors Actuators A Phys.* 332, 113173. doi:10.1016/j.sna.2021.113173
- Lee, P.-C., Peng, C.-L., and Shieh, M.-J. (2016). Combining the Single-Walled Carbon Nanotubes with Low Voltage Electrical Stimulation to Improve Accumulation of Nanomedicines in Tumor for Effective Cancer Therapy. *J. Control. Release* 225, 140–151. doi:10.1016/j.jconrel.2016.01.038
- Li, Q., Liu, W., Yang, H., He, W., Long, L., Wu, M., et al. (2021). Ultra-stability High-Voltage Triboelectric Nanogenerator Designed by Ternary Dielectric Triboelectrification with Partial Soft-Contact and Non-contact Mode. *Nano Energy* 90, 106585. doi:10.1016/j.nanoen.2021.106585
- Liu, Z., Nie, J., Miao, B., Li, J., Cui, Y., Wang, S., et al. (2019). Self-Powered Intracellular Drug Delivery by a Biomechanical Energy-Driven Triboelectric Nanogenerator. *Adv. Mat.* 31, 1807795. doi:10.1002/adma.201807795
- Macfelda, K., Kapeller, B., Holly, A., Podesser, B. K., Losert, U., Brandes, K., et al. (2017). Bioelectrical Signals Improve Cardiac Function and Modify Gene Expression of Extracellular Matrix Components. *Esc. Heart Fail.* 4, 291–300. doi:10.1002/ehf2.12169
- Qin, H., Cheng, G., Zi, Y., Gu, G., Zhang, B., Shang, W., et al. (2018). High Energy Storage Efficiency Triboelectric Nanogenerators with Unidirectional Switches and Passive Power Management Circuits. *Adv. Funct. Mat.* 28, 1805216. doi:10.1002/adfm.201805216
- Qin, H., Gu, G., Shang, W., Luo, H., Zhang, W., Cui, P., et al. (2020). A Universal and Passive Power Management Circuit with High Efficiency for Pulsed
- Supplementary Figure S1** | The integral results of the D-TENG's output current. (a) The integral result of the D-TENG's output current without any additional process, which shows the output charge pure peak. (b) The integral result of the absolute values of D-TENG's output current, which shows the total output charge.
- Supplementary Figure S2** | The integral results of the current transmitted to the tailor-made culture dish, which shows the total charge flowing through the culture solution.
- Triboelectric Nanogenerator. *Nano Energy* 68, 104372. doi:10.1016/j.nanoen.2019.104372
- Shang, W., Gu, G., Zhang, W., Luo, H., Wang, T., Zhang, B., et al. (2021). Rotational Pulsed Triboelectric Nanogenerators Integrated with Synchronously Triggered Mechanical Switches for High Efficiency Self-Powered Systems. *Nano Energy* 82, 105725. doi:10.1016/j.nanoen.2020.105725
- Su, Y., Xie, G., Tai, H., Li, S., Yang, B., Wang, S., et al. (2018). Self-powered Room Temperature NO₂ Detection Driven by Triboelectric Nanogenerator under UV Illumination. *Nano Energy* 47, 316–324. doi:10.1016/j.nanoen.2018.02.031
- Sung, H., Ferlay, J., Siegel, R. L., Laversanne, M., Soerjomataram, I., Jemal, A., et al. (2021). Global Cancer Statistics 2020: GLOBOCAN Estimates of Incidence and Mortality Worldwide for 36 Cancers in 185 Countries. *CA A Cancer J. Clin.* 71, 209–249. doi:10.3322/caac.21660
- Wang, H., Pastorin, G., and Lee, C. (2016). Toward Self-Powered Wearable Adhesive Skin Patch with Bendable Microneedle Array for Transdermal Drug Delivery. *Adv. Sci.* 3, 1500441. doi:10.1002/advs.201500441
- Wang, M., Zhang, J., Tang, Y., Li, J., Zhang, B., Liang, E., et al. (2018). Air-Flow-Driven Triboelectric Nanogenerators for Self-Powered Real-Time Respiratory Monitoring. *ACS Nano* 12, 6156–6162. doi:10.1021/acsnano.8b02562
- Wang, S., Xie, Y., Niu, S., Lin, L., Liu, C., Zhou, Y. S., et al. (2014). Maximum Surface Charge Density for Triboelectric Nanogenerators Achieved by Ionized-Air Injection: Methodology and Theoretical Understanding. *Adv. Mat.* 26, 6720–6728. doi:10.1002/adma.201402491
- Wang, T., Gu, G., Shang, W., Gan, J., Zhang, W., Luo, H., et al. (2021). A Self-Powered Photodetector Using a Pulsed Triboelectric Nanogenerator for Actual Working Environments with Random Mechanical Stimuli. *Nano Energy* 90, 106518. doi:10.1016/j.nanoen.2021.106518
- Wang, Z., Cheng, L., Zheng, Y., Qin, Y., and Wang, Z. L. (2014). Enhancing the Performance of Triboelectric Nanogenerator through Prior-Charge Injection and its Application on Self-Powered Anticorrosion. *Nano Energy* 10, 37–43. doi:10.1016/j.nanoen.2014.08.017
- Wang, Z. L. (2017). On Maxwell's Displacement Current for Energy and Sensors: the Origin of Nanogenerators. *Mater. Today* 20, 74–82. doi:10.1016/j.mattod.2016.12.001
- Wang, Z. L. (2013). Triboelectric Nanogenerators as New Energy Technology for Self-Powered Systems and as Active Mechanical and Chemical Sensors. *ACS Nano* 7, 9533–9557. doi:10.1021/nl404614z
- Weaver, C. L., LaRosa, J. M., Luo, X., and Cui, X. T. (2014). Electrically Controlled Drug Delivery from Graphene Oxide Nanocomposite Films. *ACS Nano* 8, 1834–1843. doi:10.1021/nn406223e
- Yuan, M., Li, X., Liu, J., Zheng, Y., Cheng, L., Tang, N., et al. (2021). Fully Integrated Self-Powered Electrical Stimulation Cell Culture Dish for Noncontact High-Efficiency Plasmid Transfection. *ACS Appl. Mat. Interfaces* 13, 54762–54769. doi:10.1021/acsmi.1c16748
- Zhang, C., Chen, J., Xuan, W., Huang, S., Shi, L., Cao, Z., et al. (2022). Triboelectric Nanogenerator-Enabled Fully Self-Powered Instantaneous Wireless Sensor Systems. *Nano Energy* 92, 106770. doi:10.1016/j.nanoen.2021.106770
- Zhang, L., Cheng, L., Bai, S., Su, C., Chen, X., and Qin, Y. (2015). Controllable Fabrication of Ultrafine Oblique Organic Nanowire Arrays and Their Application in Energy Harvesting. *Nanoscale* 7, 1285–1289. doi:10.1039/c4nr06237j
- Zhang, R., Hao, M., Bai, S., Song, P., Jia, X., Gao, W., et al. (2022). Multichannel Driving Triboelectric Nanogenerator for Enhancing the Output Charge Density. *Nano Energy* 98, 107272. doi:10.1016/j.nanoen.2022.107272
- Zhang, W., Gu, G., Qin, H., Li, S., Shang, W., Wang, T., et al. (2020). Measuring the Actual Voltage of a Triboelectric Nanogenerator Using the Non-grounded Method. *Nano Energy* 77, 105108. doi:10.1016/j.nanoen.2020.105108
- Zhang, W., Gu, G., Shang, W., Luo, H., Wang, T., Zhang, B., et al. (2021). A General Charge Compensation Strategy for Calibrating the Voltage of a Triboelectric

- Nanogenerator Measured by a Capacitive Circuit. *Nano Energy* 86, 106056. doi:10.1016/j.nanoen.2021.106056
- Zhang, Y., Gao, X., Wu, Y., Gui, J., Guo, S., Zheng, H., et al. (2021). Self-powered Technology Based on Nanogenerators for Biomedical Applications. *Exploration* 1, 90–114. doi:10.1002/EXP.20210152
- Zhang, Z., Qiu, S., Zhang, X., and Chen, W. (2018). Optimized DNA Electroporation for Primary Human T Cell Engineering. *BMC Biotechnol.* 18, 4. doi:10.1186/s12896-018-0419-0
- Zhao, C., Feng, H., Zhang, L., Li, Z., Zou, Y., Tan, P., et al. (2019). Highly Efficient *In Vivo* Cancer Therapy by an Implantable Magnet Triboelectric Nanogenerator. *Adv. Funct. Mat.* 29, 1808640. doi:10.1002/adfm.201808640
- Zhao, K., Gu, G., Zhang, Y., Zhang, B., Yang, F., Zhao, L., et al. (2018). The Self-Powered CO₂ Gas Sensor Based on Gas Discharge Induced by Triboelectric Nanogenerator. *Nano Energy* 53, 898–905. doi:10.1016/j.nanoen.2018.09.057
- Zheng, Q., Zhang, H., Shi, B., Xue, X., Liu, Z., Jin, Y., et al. (2016). *In Vivo* Self-Powered Wireless Cardiac Monitoring via Implantable Triboelectric Nanogenerator. *ACS Nano* 10, 6510–6518. doi:10.1021/acsnano.6b02693
- Zheng, Y., Cheng, L., Yuan, M., Wang, Z., Zhang, L., Qin, Y., et al. (2014). An Electrospun Nanowire-Based Triboelectric Nanogenerator and its Application in a Fully Self-Powered UV Detector. *Nanoscale* 6, 7842–7846. doi:10.1039/c4nr01934b
- Zheng, Y., Ma, S., Benassi, E., Feng, Y., Xu, S., Luo, N., et al. (2022). Surface Engineering and On-Site Charge Neutralization for the Regulation of Contact Electrification. *Nano Energy* 91, 106687. doi:10.1016/j.nanoen.2021.106687
- Zhong, L., Li, Y., Xiong, L., Wang, W., Wu, M., Yuan, T., et al. (2021). Small Molecules in Targeted Cancer Therapy: Advances, Challenges, and Future Perspectives. *Sig Transduct. Target Ther.* 6, 1–48. doi:10.1038/s41392-021-00572-w

Conflict of Interest: The authors declare that the research was conducted in the absence of any commercial or financial relationships that could be construed as a potential conflict of interest.

Publisher's Note: All claims expressed in this article are solely those of the authors and do not necessarily represent those of their affiliated organizations or those of the publisher, the editors, and the reviewers. Any product that may be evaluated in this article, or claim that may be made by its manufacturer, is not guaranteed or endorsed by the publisher.

Copyright © 2022 Chen, Deng, He, Cheng, Ren and Xu. This is an open-access article distributed under the terms of the Creative Commons Attribution License (CC BY). The use, distribution or reproduction in other forums is permitted, provided the original author(s) and the copyright owner(s) are credited and that the original publication in this journal is cited, in accordance with accepted academic practice. No use, distribution or reproduction is permitted which does not comply with these terms.